

AD-A059 798

UNIVERSITY OF SOUTHERN CALIFORNIA LOS ANGELES DEPT O--ETC F/G 20/4
THEORY OF OBLIQUE WINGS OF HIGH ASPECT RATIO.(U)

AUG 78 H K CHENG

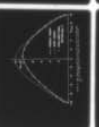
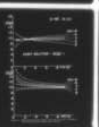
N00014-75-C-0520

UNCLASSIFIED

USCAE-135

NL

1 OF 1
AD
A059798



END
DATE
FILMED
12-78

DDC

AD A059798

DDC FILE COPY

LEVEL

USCAE 135
August 1978



12

UNIVERSITY OF SOUTHERN CALIFORNIA

SCHOOL OF ENGINEERING

THEORY OF OBLIQUE WINGS OF HIGH ASPECT RATIO

H. K. Cheng



Office of Naval Research
Contract No. N00014-75-C-0520
Identification Number NR 061-192

DEPARTMENT OF AEROSPACE ENGINEERING

"Approved for public release; distribution unlimited."

Engineering

14
USCAE-135

11
AUG 1978

12 457

6 THEORY OF OBLIQUE WINGS OF HIGH ASPECT RATIO.

10 H. K. Cheng

9 Technical rept.,

15

Office of Naval Research

Contract No. N00014-75-C-0520

Identification Number NR 061-192

Department of Aerospace Engineering
University of Southern California
Los Angeles, California

402 019

not

THEORY OF OBLIQUE WINGS OF HIGH ASPECT RATIO

H.K. Cheng
University of Southern California
Los Angeles, California 90007

ABSTRACT

The aerodynamic characteristics of oblique wings in an inviscid, incompressible flow, linearized for small wing camber and incidence, is studied under the assumption that the wing aspect ratio R_1 is high. Apart from the addition of a dominant upwash correction of the order $R_1^{-1/2} \ln R_1$, resulting from the sweep of the center line, the present analysis differs from the classical lifting-line theory in that the flow field next to the wing section (the inner solution) is affected by a component of the wake vorticity parallel to the center line, and, hence, is not locally two-dimensional. A crucial aspect of the analysis involves the behavior of the three-dimensional corrections near the leading and trailing edges, which require special attention, lest nonuniformities arise. The results determined from matching the inner and outer solutions exhibit a strong asymmetrical spanwise influence of the wake vorticities, with a lift increase on the downstream wing panel and a lift reduction on the upstream panel. Results obtained are compared with surface-lift distributions generated by an inversed method for yawed elliptic planforms, and with span loadings generated by a panel method for elliptic flat plates (wings with zero camber) as well as an ESP (extended-span planform) wing. For R_1 in the range of 10 to 20, good agreement in the comparison is consistently found, and the improvement over the strip (local 2-D) theory is shown to be great. Recast into a rational fraction (in a form similar to that used originally by Prandtl), results obtained can be improved further and shown to be adequate for aspect ratio down to at least $R_1 = 4.33$ corresponding to a 5:1 ellipse at 30° yaw. The report also furnishes computed (finite-part of the) upwash data which will be useful in other related subsonic and transonic applications.

ACCESSION for		Wing Section <input checked="" type="checkbox"/>
NTIS		S.M. Section <input type="checkbox"/>
DDC		
UNANNOUNCED		
JUSTIFICATION		
BY DISTRIBUTION/AVAILABILITY CODES		
Dist.	Avail. & C.	SP. CIAL
A		

1. INTRODUCTION

The effect of far-wake vorticities is essential in any analysis of three-dimensional (3-D) lifting surfaces. In Prandtl's (1918) lifting-line theory of a high-aspect-ratio wing, the calculation of this effect is greatly simplified by replacing the wing with a line of singularity comprising all bound vortices. A restriction in Prandtl's work, as well as the more systematic, asymptotic theory of Van Dyke (1964) and Ashely and Landahl (1965), is the assumption that the wing center line (a reference curve in the theory) is straight and unswept (being perpendicular to the main flow). The present study considers extensions of this approach to planar wing problems, in which the afore mentioned restriction is removed. The primary purpose of this note is to point out certain distinct features of such a theory, concentrating mainly on the development for a steady incompressible potential flow past an oblique wing (of which the center line may be taken as being straight). Comparison with results of more exact calculations by other methods will be made.

The work reported represents a special case of the theory of high-aspect-ratio wings involving curved center lines; while the analysis is simplified owing to the absence of the center-line curvature, a few of the basic features brought out below remain crucial ingredients in the more general theory to follow. An abridged version of this work has been made in the form of a technical note (Cheng 1978). Apart from a fuller presentation and discussion of the theory, this report gives additional comparisons of the theory with the panel method in the lower aspect-ratio range and for an ESP oblique wing not previously considered.

Among earlier methods employing the lifting-line idea to swept wings, (see, for example , Jones and Cohen, 1957), the most well known is, perhaps, that of Weisinger (1942), which fails, however, in the limit of an infinite aspect ratio. Solutions to elliptic lifting surfaces at yaw have been given early by Krienes (1940), based on a superposition of products involving Lamé's functions. Readers are referred to Jones and Cohen (1957) for a helpful delineation of Krienes' analysis, where applications of certain results for unyawed elliptic planforms are made. Krienes treated the direct problem for an elliptic flat plate, and obtained results for an 5:1 ellipse at $0-30^{\circ}$ yaw. Of the five-term truncated series used therein, three terms were symmetric spanwise, it is not clear if the remaining terms would adequately delineate the asymmetric span load of interest. Generalization of the lifting-line theory for a wing with a curved center line, as well as a wing in side slip, has been made by Dorodnitsyn (1944), who noted the significance of the logarithmically large upwash due to yaw. However, the analysis involved an ad hoc treatment in which the lifting surface is replaced by a lifting line at the quarter-chord location and the resulting upwash correction is evaluated at the three-quarter-chord location. The result was, in any case, restricted to small departures from a straight, unswept center line.

A case of curved center line has been studied by Thurber (1965) who considered a crescent-moon-shaped wing from the view point of asymptotic methods; but the inner solution and the matching problem were not considered (the upwash calculation also contained errors). Oscillating high-aspect-ratio wings with curved center lines have been treated by the author

(Cheng 1976); however, upwash calculation for the low-frequency and quasi-steady cases has not been given, and the formal inner solution presented therein is incomplete (see below). Apart from the hope of gaining physical insights and simplicity for analyzing transonic oblique wings and animal swimming propulsion (Jones 1972, 1977; Lighthill 1975; Chopra and Kambe 1977; Cheng 1976), the present asymptotic approach has been motivated by a desire to implement the current computer-oriented 3-D methods which, though very powerful, are by no means free from both cost and storage limitations (see Bauer, Garabedian, Korn and Jameson 1974, Jameson and Caughey 1977, Ashley and Rodden 1972). Problems involving curved center lines in steady and unsteady flows will be treated fully in separate papers. Extension to transonic flow problems involving nonlinear component flow have been studied by Cheng and Meng (1978, 1978b).

2. PRELIMINARY REMARKS

In Prandtl's theory,¹ the 3-D effects appear mainly as a local incidence correction and can be calculated readily as one half of the upwash at the wing trace in the Trefftz plane. This simplicity is lost, if the center line has a nonvanishing sweep angle or curvature; the solution in this case cannot be unambiguously determined without recourse to a more systematic analysis employing matched asymptotic expansions. Certain features of the theory absent in the classical works are noteworthy and may be inferred from rather elementary considerations. As will be seen below, most of these features may be traced to the presence of a spanwise component of the local wake vorticity.

Logarithmic upwash

The most obvious among these features is perhaps the dominant induced upwash resulting from the sweep. From the view point of an asymptotic theory, this additional upwash is significant in that it adds terms of the order $R_1^{-1} \ln R_1$ to corrections which are otherwise of the order R_1^{-1} , where R_1 is an appropriately defined aspect ratio to be given later. As pointed out by Cheng (1976), the wake vorticity $d\Gamma/dy$ (using Prandtl's notation) shed locally has a component along the swept center line, which gives rise to a logarithmically singular upwash near the center (lifting) line. Therefore, this raises the magnitude of the upwash in the inner-flow region next to the wing by a factor of $\ln R_1$.

The near-wake influence

With a nonvanishing spanwise component of the wake vorticities, the flow region next to the wing section can no longer be well represented by

wakeless 2-D divergence-free flow as in most classical analyses. Thus, in addition to the upwash induced by the far wake (to be determined by matching), the inner solution must properly account for the upwash at the upper and lower airfoil surfaces induced by this component of the vorticity right behind the trailing edge (which, to the leading order, is proportional to the local value of $\sin \Lambda \cdot dP/dy$).

Problems of edge singularities: nonuniformities

As in most classical lifting-surface theory dealing with a direct problem, in which a finite upwash (slope of the camber surface) is prescribed over the wing, it is required that the singularity of the velocity at the leading edge and trailing edge be no stronger than $\rho^{-1/2}$ and $\rho^{1/2}$, respectively. In above, ρ stands for distance from the edge. For wing upwash which becomes logarithmically infinite at the edges like $\ln \rho$, it will be required that the nearby velocity field behaves no worse than $\ln \rho$. At the leading edge, these requirements may be alternatively replaced by one requiring integrability (with respect to distance) of the surface pressure or surface speed. At the trailing edge, the requirement is equivalent to the Kutta-Joukowski condition.

In constructing analytic solutions to the reduced problems in the asymptotic theory for large R , it is essential to adhere to the foregoing conditions at successive orders of R , the requirements tantamount to enforcing uniform validity of the expansion at both edges. This is so because partial derivatives with respect to distance along the center line, say $\partial/\partial y'$, appear in certain equations, which would raise the order of an algebraic or logarithmic singularity, unless the location

of the singularity is independent of y' (see Section 4 below). Homogeneous solutions with proper singular behaviors must be added when necessary to fulfill the stated requirements and to avoid nonuniformity.

We note in passing that an additional logarithmic upwash appears if the relative wing motion is unsteady, or if the center line curvature is comparable to the reciprocal of the span.

3. COORDINATES AND DESCRIPTION OF THE FULL PROBLEM

The following analysis, employs two right-handed Cartesian system. In (x,y,z) system, the reference wing plane is $z = 0$ and makes an angle of attack α_0 with the undisturbed flow; thus, the velocity vector at the infinity appears in this system as $(U \cos \alpha_0, 0, U \sin \alpha_0)$, where U is the free-stream speed. The second system (x',y',z') is generated from the first by a rotation about the z -axis (cf. Fig. 1).

$$x' = \cos \Lambda x - \sin \Lambda y, \quad y' = \sin \Lambda x + \cos \Lambda y, \quad z = z'. \quad (3.1)$$

The y' -axis is taken as the center line of the oblique wing. Note that the wing planes lies in $z' = z = 0$ and that Λ is the sweep angle. The variables x' and z' are normalized by the root chord c_0 (measured parallel to x' axis); y' , along with x, y and z , are normalized by the half span b . The primed system is employed to describe the inner region near the wing section and the unprimed one for the outer region.

The perturbation potential ϕ of the full linearized problem must satisfy the 3-D Laplace equation, being regular everywhere except in approaching the wing and the trailing vortex sheet; it must also vanish at the infinity except near the far wake. In approaching the upper and lower surfaces, $z = z_w(x,y)$, the linearized impermeability condition, transferred to the wing plane $z = 0$, is

$$\left(\frac{\partial \phi}{\partial z} \right)_w = U \frac{\partial z_w}{\partial x} - \alpha_0 \quad (3.2a)$$

and in approaching the trailing vortex (TV) sheet, the continuity of pressure and normal velocity requires

$$\left[\left[\frac{\partial \phi}{\partial x} \right] \right]_{TV} = \left[\left[\frac{\partial \phi}{\partial z} \right] \right]_{TV} = 0 \quad (3.2b)$$

where the subscript **w** and **TV** signify the wing and the trailing-vortex sheet, respectively, and the double bracket $\left[\left[\right] \right]$ stands for differences across the wing or the TV sheet. The velocity is allowed to be unbounded at the leading edge but must be integrable; the pressure or ϕ_x on the wing is required to remain bounded at the trailing edge so that the Kutta condition is satisfied.

We observe in passing that, the free-stream velocity vector could be alternately set to be $(U, 0, 0)$, along with the omission of $-\alpha_o$ from Eq. (3.2a) (note that $\partial z_w / \partial x$ in this alternative system differs from that in the original (x, y, z) system by $-\alpha_o$). This alternative system with the free-stream velocity as $(U, 0, 0)$ has been used in Cheng (1978) and is equivalent to the (x, y, z) system adopted in the present work, for all practical purposes. The present (x, y, z) system with $(U \cos \alpha_o, 0, U \sin \alpha_o)$ is preferred, as it avoids a conceptual difficulty which one would encounter in the transfer of the wing boundary condition to the wing plane ($z = 0$) in the case of a high-aspect-ratio wing when the angle of attack is comparable to R_i^{-1} .

Throughout the development in Sections 4 and 5, an aspect ratio defined as $R_i \equiv 2b/c_o$ is used. Note that the distance from tip to tip $2l$ is less than the span $2b = 2l \cdot \cos \Lambda$. Another aspect ratio $R_o \equiv 2l/c_o = R_i \sec \Lambda$ will be used later for the convenience in comparing results for the same wing at different sweep angles. The aspect

ratio R_1 is preferred, as the theory developed requires

$$C_0/2b = R_1^{-1} \ll 1 \quad (3.3)$$

which is significantly different from $C_0/2l = R_0^{-1} \ll 1$. The parameter controlling wing camber and incidence, including the angle α_0 , is denoted by ϵ . The wing ordinate z_w normalized by ϵC_0 , is written as $Z(x', y')$.

ERRATA

"THEORY OF OBLIQUE WINGS OF HIGH ASPECT RATIO"

USCAE 135

By H. K. Cheng

Page 8, Eq. (3.2a): change " $\oint \frac{\partial \tilde{\gamma}}{\partial x} = \alpha_0$ " to " $\oint \left(\frac{\partial \tilde{\gamma}}{\partial x} - \alpha_0 \right)$."

Page 11, First line after Eq. (4.3a,b,c): change " $\tilde{\alpha}_0 = -\alpha_0/\epsilon$ " to " $\tilde{\alpha}_0 = -\alpha_0/\epsilon \cos \Lambda$ ".

Page 26, In the reference of Cheng and Meng (1978a): change "submitted to" to "accepted for publication in".

78 10 06 041

4. INNER PROBLEM

The linearized problem under a small ϵ admits a development for high aspect ratio (for finite x', y', z')

$$\phi' \equiv \frac{\phi}{\epsilon C_0 U \cos \Lambda} = \phi_0 + \mathcal{R}_1^{-1} \phi_1 + \mathcal{R}_1^{-2} \phi_2 + \dots \quad (4.1)$$

allowing a weak logarithmic dependence of ϕ_1 and ϕ_2 on \mathcal{R}_1 . The first two terms satisfy the 2-D Laplace equation in x' and z' . The conditions on the wing and the vortex sheet, Eqs. (3.2), through the transform Eq. (3.1), yield

$$\left(\frac{\partial \phi_0}{\partial z'} \right)_w = \frac{\partial}{\partial x'} Z - \tilde{\alpha}_0, \quad \left[\frac{\partial \phi_0}{\partial x'} \right]_{TV} = 0, \quad \left[\frac{\partial \phi_0}{\partial z'} \right]_{TV} = 0; \quad (4.2 \text{ a,b,c})$$

$$\left(\frac{\partial \phi_1}{\partial z'} \right)_w = 2m \frac{\partial}{\partial y'} Z, \quad \left[\frac{\partial \phi_1}{\partial x'} \right]_{TV} = -2m \left[\frac{\partial \phi_0}{\partial y'} \right]_{TV}, \quad \left[\frac{\partial \phi_1}{\partial z'} \right]_{TV} = 0 \quad (4.3 \text{ a,b,c})$$

where $m = \tan \Lambda$, and $\tilde{\alpha}_0 = -\alpha_0/\epsilon$; $2m \left[\frac{\partial \phi_0}{\partial y'} \right]_{TV}$ results from the component of trailing vorticity parallel to the center line.

The solution ϕ_0 satisfying the boundary conditions (4.2), fulfilling the edge conditions mentioned, and yielding a zero disturbance velocity at large $x'^2 + z'^2$, is provided by the classical 2-D thin airfoil theory. As it is well known, the vorticity strength $\left[\partial \phi_0 / \partial x' \right]$ on the wing is a solution to the integral equation ($a' < x' < b'$)

$$\frac{1}{2\pi} \text{P.V.} \int_{a'}^{b'} \frac{\left[\partial \phi_0 / \partial x_i \right]}{x_i' - x'} dx_i' = \frac{\partial}{\partial x'} Z - \tilde{\alpha}_0 \quad (4.4)$$

where P.V. signifies the Cauchy principal value; a' and b' locate the leading and trailing edges, respectively.

The solution ϕ_i which meets the same edge singularity requirements and allows matching with the outer solution can be obtained as the sum

$$\phi_i = \varphi + \varphi^P + V_1^\infty z' \quad (4.5)$$

where V_1^∞ is an anticipated upwash correction to be determined by matching later; φ^P is a (particular) solution satisfying the (nonhomogeneous) TV boundary conditions in Eq. (4.3b), and φ is a (wakeless) 2-D thin airfoil solution with its wing upwash so chosen to make ϕ_i fulfilling Eq. (4.3a). The solution φ^P can be obtained as

$$\varphi^P = -2m \text{R.P.}(\xi \partial W / \partial \gamma') + \varphi_H^P \quad (4.6)$$

where R.P. signifies the real part, ξ is the complex variable $x' + iz'$, W is the complex potential $\phi_0 + i\psi_0$; φ_H^P is a wakeless harmonic function (not considered in Cheng 1978), needed to keep φ^P , hence ϕ_i , from becoming more singular than ϕ_0 at the edges (see below). To fulfill Eq. (4.3a), the jump in $\partial\varphi/\partial x'$ across the wing must satisfy the same integral equation as Eq. (4.4), with the R.H.S. replaced however, by

$$V_i \equiv 2m \partial Z / \partial \gamma' + 2m x' \partial^2 Z / \partial \gamma' \partial x' - (\partial \varphi_H^P / \partial z')_\omega + 2m \frac{\partial}{\partial \gamma'} (Z - Z_{LE} - \psi_{0LE} + \tilde{\alpha}_0 \alpha') - V_1^\infty. \quad (4.7)$$

In the absence of the Kutta condition, the φ_H^P , together with the part of φ contributed by $-(\partial \varphi_H^P / \partial z')_\omega$ in V_i above would belong to the family of eigensolutions for ϕ_i .

In choosing φ_H^P , one notes that the singular behavior of ϕ_i is dominated by the first member of φ^P in Eq. (4.6) as $2ma'(\partial a' / \partial \gamma') \partial W / \partial \xi$ at the leading edge and $2mb'(\partial b' / \partial \gamma') \partial W / \partial \xi$ at the trailing edge. For cases wherein the camber slope is nowhere infinite, it suffices to take

$$\varphi_H^P = 2m\alpha' \frac{\partial \phi_0}{\partial y'} + 2m\sqrt{C'} E \frac{db'}{dy'} R.P. \left[i(\xi - a')^{1/2} (\xi - b')^{1/2} - i\xi \right] \quad (4.8)$$

where E is the coefficient in $\partial \phi_0 / \partial x' \sim E(b' - x')^{1/2}$. For the case with infinite camber slopes at the edges, the prescription is

$$\varphi_H^P = 2m\alpha' \frac{\partial}{\partial y'} \phi_0^{LE} + 2mb' \frac{\partial}{\partial y'} \phi_0^{TE} \quad (4.9)$$

where ϕ_0^{LE} is a solution of the ϕ_0 type, with its x' -derivative tending to $\partial \phi_0 / \partial x'$ at L.E. and vanishing no less rapidly than $(b' - x')$ at T.E.; ϕ_0^{TE} is similar, with supercript L.E. replace by T.E. and a' by b' . An important example for this case is logarithmically infinite cambers supporting finite pressure jumps at the edges.

In terms of the pressure coefficient C_p' based on the dynamic pressure of the component flow, the pressure jump across the wing can be obtained from

$$[[C_p']] / 2\varepsilon = -\frac{\partial}{\partial x'} [[\phi_0]] - R_i^{-1} \left[\left[\frac{\partial}{\partial x'} \varphi - 2mx' \frac{\partial^2}{\partial y' \partial x'} \phi_0 + \frac{\partial}{\partial x'} \varphi_H^P \right] \right] \quad (4.10)$$

The span loading is ρU times the potential jump at the trailing edge at the y -(spanwise) station and can be computed from the jumps in ϕ_0 , φ and φ_H^P at the trailing edge at the corresponding y' -station; in normalized form

$$\begin{aligned} S.L. &\equiv 2b\rho U [[\phi]]_{TE} / \frac{1}{2}\rho U^2 S_w = \\ &= 4bc_0 S_w^{-1} \varepsilon \cos \Lambda \left[[\phi_0 + R_i^{-1}(\varphi + \varphi_H^P)] \right]_{TE}. \end{aligned} \quad (4.11)$$

In the outer limit $|\xi| \rightarrow \infty$, the inner solution becomes

$$\begin{aligned}
\phi' \sim (2\pi)^{-1} \Pi'(y') & \left[\tan^{-1}(x'/z') + \frac{\pi}{2} \operatorname{sgn} z' \right] - (2\pi)^{-1} \int_{a'}^{b'} [\![\phi'_0]\!] x'_i dx'_i R.p.(i\xi^{-1}) + \\
& + R_i^{-1} \pi^{-1} m \frac{d\Pi'_0}{dy'} z' \ln|\xi| - R_i^{-1} \pi^{-1} m \frac{d\Pi'_0}{dy'} x' \left[\tan^{-1}(x'/z') + \frac{\pi}{2} \operatorname{sgn} z' \right] + \\
& + R_i^{-1} V_i^\infty z' + O(z' \xi^{-1} R_i^{-1}, R_i^{-2}),
\end{aligned} \tag{4.12}$$

where Π'_0 stands for $[\![\phi'_0]\!]_{TE}$, and $\Pi'(y') = \Pi'_0(y') + R_i^{-1} [\![\varphi + \varphi_N^P]\!]_{TE}$.

5. OUTER PROBLEM AND MATCHING

In flow region removed from the wing sections, the spatial variation is scaled by $b \gg c_0$, and the solution may be represented to the leading order by concentrated vortices with circulation $\Gamma_0(y)$ bounded to the center line, together with the trailing vortex sheet. The perturbation potential for this outer problem is then $\Phi = \Phi_0 + \mathcal{R}_1^{-1} \Phi_1 + \dots$, with

$$\Phi_0(x, y, z) = \frac{1}{4\pi} \int_{-1}^1 \frac{\Gamma_0(y_1)}{(y-y_1)^2 + z^2} \left[1 + \frac{x-my_1}{\sqrt{(x-my_1)^2 + (y-y_1)^2 + z^2}} \right] dy_1 \quad (5.1)$$

anticipating the determination of Γ_0 by matching, both Γ_0 and Φ_0 in Eq. (5.1) are normalized by $\varepsilon c_0 U \cos \Lambda$ (same as for Π' and Φ').

In approaching the center line ($\xi \equiv x-my \rightarrow 0, z \rightarrow 0$) the integrand shown in Eq. (5.1) becomes singular at $u \equiv y_1 - y = 0$ like

$$g(\xi, y, z; u) = \frac{\Gamma(y) + \Gamma'(y)u}{u^2 + z^2} \left[1 + \frac{\xi - mu}{R_u} \right] \quad (5.2)$$

where $R_u \equiv \sqrt{(1+m^2)u^2 + 2m\xi u + \xi^2 + z^2}$. By subtraction of terms shown above from the integrand, the resulting integral then has a (finite) limit as ξ and z vanish. This, together with the quadrature of g , gives the inner limit sought

$$\begin{aligned} \Phi \sim & \frac{\Gamma_0(y)}{2\pi} \cdot \left[\tan^{-1}(\xi/\sqrt{1+m^2}z) + \frac{\pi}{2} \operatorname{sgn} z \right] - \\ & - \frac{z}{4\pi\sqrt{1+m^2}} \cdot \Gamma_0'(y) \cdot \left[\ln \left| \frac{4(1+m^2)^2(1-y^2)}{\xi^2 + (1+m^2)z^2} \right| + 2 \right] + \\ & + \frac{z}{4\pi} \cdot \Gamma_0'(y) \cdot \ln \left| \frac{1-y}{1+y} \frac{m+\sqrt{1+m^2}}{m-\sqrt{1+m^2}} \right| + \end{aligned}$$

$$+ \frac{z}{4\pi} \int_{-1}^1 \frac{\Gamma'_0(y_1) - \Gamma'_0(y)}{y_1 - y} \left[1 - \frac{m}{\sqrt{1+m^2}} \operatorname{sgn}(y_1 - y) \right] dy_1 + \quad (5.3)$$

$$+ O((\xi + z)^2, S^{-1} R_i^{-1}),$$

where $O(S^{-1} R_i^{-1})$ is expected to arise from $R_i^{-1} \bar{\Phi}$. In terms of the inner variables $x' = z^{-1} R_i \cos \Lambda \xi$, $z' = z^{-1} R_i z$, and observing that $\Gamma'_0(y) = \Gamma'_0(y' \cos \Lambda) - 2m R_i^{-1} x' \frac{d\Gamma_0}{dy}$, Eq. (5.3) can be expressed as

$$\begin{aligned} \bar{\Phi} \sim & \frac{1}{2\pi} \Gamma_0(y' \cos \Lambda) \cdot \left[\tan^{-1}\left(\frac{x'}{z'}\right) + \frac{\pi}{2} \operatorname{sgn} z' \right] - \\ & - \frac{1}{\pi} m R_i^{-1} x' \frac{d\Gamma_0}{dy} \left[\tan^{-1}\left(\frac{x'}{z'}\right) + \frac{\pi}{2} \operatorname{sgn} z' \right] + \\ & + \frac{1}{\pi} m R_i^{-1} z' \frac{d\Gamma_0}{dy} \ln|\xi| + \\ & + 2 R_i^{-1} z' \Gamma_0(0) \Sigma(y') + O(R_i^{-2} |\xi|^2, S^{-1}, R_i^{-1}) \end{aligned} \quad (5.4a)$$

where $\Sigma(y)$ is the upwash function in y (not y')

$$\begin{aligned} \Sigma(y) \equiv & -\frac{1}{2\pi} \sin \Lambda \bar{\Gamma}'_0(y) \ln(R_i) + \\ & + \frac{1}{4\pi} \bar{\Gamma}'_0(y) \left[\ln \left| \frac{1-y}{1+y} \frac{(1+\sin \Lambda)^2}{\cos^2 \Lambda} \right| - \sin \Lambda \left(2 + \ln \left| \frac{1-y^2}{\cos^2 \Lambda} \right| \right) \right] + \\ & + \frac{1}{4\pi} \int_{-1}^1 \frac{\bar{\Gamma}'_0(y_1) - \bar{\Gamma}'_0(y)}{y_1 - y} \left[1 - \sin \Lambda \operatorname{sgn}(y_1 - y) \right] dy_1, \end{aligned} \quad (5.4b)$$

and $\bar{\Gamma}_0(y) = \Gamma_0(y) / \Gamma_0(0)$, $\bar{\Gamma}'_0 = d\bar{\Gamma}_0/dy$.

Eqs. (4.12) and (5.4) are valid expansions of R_i^{-1} in the common domain

$1 \ll |\xi| \ll R_i$, where the inner and outer solutions can be matched, provided one makes the identifications

$$\Gamma_0(y' \cos \Lambda) = \Pi_0(y'), \quad V_i^\infty = 2 \Gamma_0(0) \Sigma(y). \quad (5.5)$$

The upwash correction, hence the inner solution to the order R_i^{-1} , is now determined.

It is useful to point out that $R_i^{-1} V_i^\infty$ is the finite part of the local induced flow angle α_i divided by ξ , and that Σ is $R_i \alpha_i$ divided by the sectional lift coefficient at $y = 0$. The first term in Eq. (5.4b) corresponds to the logarithmic upwash mentioned earlier which dominates the

finite part of the induced velocity, increasing the upwash on the aft panel (where $d\Gamma_0/dy < 0$) and reducing it on the forward panel (where $d\Gamma_0/dy > 0$). For Γ_0 -distributions of interest, $d\Gamma_0/dy$ behaves near $y = \pm 1$ like $(1 - y^2)^{-1/2}$, this together with the logarithm involving R_1 and $(1 - y^2)$, leads to a Σ maximum near the downstream tip at $1 - y = O(R_1^{-1})$ where the induced upwash arises from $O(R_1^{-1} \ln R_1)$ to $O(R_1^{-1/2})$. There is also a minimum in Σ near the upstream tip at $1 + y = O(R_1^{-1})$, where the induced downwash has a magnitude of $O(R_1^{-1/2})$. Although the magnitude of the induced velocity becomes infinity at the tips, Σ reverses its sign and vanishes on each wing panel at a span station extremely close to the tips. This tends to provide a reasonable description of the span loading near the tip, in spite of the local breakdown.

6. ILLUSTRATION OF THE UPWASH RESULT

Figure 2 illustrates the spanwise Σ distribution for an elliptic load $\bar{T}_0 = \sqrt{1-\gamma^2}$ and an ESP load

$$\bar{T}_0 = \sqrt{1-\gamma^2} - 0.62069 \cdot \gamma^2 \cdot \ln \left| \frac{1 + \sqrt{1-\gamma^2}}{\gamma} \right|. \quad (6.1)$$

The latter distribution has been adopted in an oblique-wing design study by Black, Beamish and Alexander (1975), and, pertains to the optimum span load for minimum induced drag with given lift under a fixed wing-root bending moment (Jones 1950). For a bending moment less than that of the elliptic load, the wing must have a longer span. A planform based on this load (assuming a zero camber) has been referred to as an extend-span planform (ESP). The ESP load shown in Eq. (6.1) and referred to in Fig. 2 corresponds to a particular ratio of the extended span to the original span taken as 1.15. Results are shown for the swept angle $\Lambda = 0, 22.5^\circ$ and 45° with a particular aspect ratio

$$R_0 = 2l/c_0 = 8.3906. \quad (6.2)$$

Since $R_1 = R_0 \cos \Lambda$ appears only through $\ln R_1$ in Σ , cf. Eq. (5.4b), the graphs can be used for other aspect ratio by simply adding to Σ *

$$-\frac{1}{2\pi} \sin \Lambda \cdot \bar{T}_0'(y) \cdot \ln \left(\frac{R_0}{8.3906} \right). \quad (6.3)$$

*

It is useful to note that if a length scale $c_s = c_0/\sigma$ other than the root chord c_0 is used for the inner solution, no alteration is needed in the above analysis, except changing R_1 to σR_1 . The relation $\Sigma = R_1 \alpha_i / c_L^{2-D} \gamma=0$ is unaffected.

Figure 2 shows that the departure from the unyawed upwash distribution is always antisymmetric (in y), and is considerably larger in the elliptic cases (broken line). Interestingly, the degree of spanwise nonuniformity in y is much greater for the ESP load (full line), varying from 0.4 at the center to 1.10 at $y = 0.9$. This is because the unyawed result of Σ for the ESP load is itself highly nonuniform spanwise. In passing, it may be noted that the exact Σ for ESP for $\Lambda = 0$ is a linear upwash distribution (Jones 1950)

$$\Sigma \propto C_1 + C_2|y|$$

(marked in thin dashes, in Fig. 2), which is recovered reasonably well by a numerical procedure applying to the ESP load of Eq. (5.6). The discrepancy shown indicates the level of accuracy to be expected in the subsequent spanload calculation for the ESP case for $\Lambda \neq 0$.

7. COMPARISONS WITH OTHER SOLUTIONS

In the following, comparisons are made of the present analysis with exact solutions derived from an inverse method and with results from a panel method.

7.1 Uniformly Loaded Oblique Wings

Wing upwash (slope) supporting a given lift distribution can be determined with relative ease; for a uniform distribution, the task reduces to evaluating a line integral. Upwash calculation has been made for several planforms with uniform load in this manner to furnish a basis for assessing the theory. Using the upwash data as an input, $[[C_p']]$ is computed by the present theory and then compared to the exact (uniform) load. This provides a test of the theory as a direct method. Of all examples considered with $R_\infty \equiv 2l/c_o = 10$ to 40 and $\Lambda = 0$ to 45° , a useful feature is that, over most parts of the wing, the upwash can be very closely represented by (with $c' = b' - a'$)

$$V_o(x', y') = \left(A(y') + B(y') \frac{x' - a'}{c'} \right) \cdot \ln \left(\frac{b' - x'}{x' - a'} \right) + C(y') \quad (7.1)$$

where B and C are generally small and decrease with increasing aspect ratio. This fact is utilized to expedite the $[[C_p']]$ computation. Figure 3 presents chordwise lift distributions at several spanwise stations computed from such an upwash over a 20:1 elliptic planform at 45° yaw, for which the exact $[[C_p']]$ has a normalized value unity (a similar result has been presented in Cheng's (1978) note for a different yaw angle, $\Lambda = 22.6^\circ$). Good agreement with the exact value (unity) is seen at the inboard stations. This represents a great improvement over $[[C_p^{(0)}]]$ from the

strip theory (lower graph) which has an error of typically 5 to 20%. Near the tips ($y/b \rightarrow \pm 1$), the lifting-line solutions deteriorates, as expected. At the 80% station (dash curves), signs of breakdown appear near the L.E., which is partly caused by the inadequacy of curve fitting based on Eq. (17) near the tip. However, the span loading (not shown) appears to remain satisfactory even at the 80% span station. Other examples with a lower aspect ratio ($R_o = 10$), as well as non-uniform lift distributions, have been studied; except for a slightly larger discrepancy near the tips, similar conclusions can be drawn for those cases. We shall return to the question on applicability of the present work to wings of lower aspect ratios later in Section 7.3.

7.2 Oblique Flat Wings

Vortex-lattice and wing-panel methods have proven adequate in many linear lifting-surface problems,[†] but their application to oblique wings does not appear to exist in the literature. The data by panel method used in the following comparison (provided by Mr. Ronald Smith) are generated from a computer program at NASA Ames Research Center, based on an extension of Woodward's (1973) method applied originally to symmetric planforms. Figure 4 presents a comparison in span loading for an elliptic flat-plate wing of $R_o = 16.78$ with a straight 40% chord line at 45° yaw. For elliptic flat plates, the theory gives a span loading in terms of elementary functions

$$\begin{aligned} S.L. / b \cos \Lambda = & \sqrt{1-y^2} - \frac{1}{R_1} \sqrt{1-y^2} \left(\frac{\pi}{2} + \sin \Lambda \sin^{-1} y \right) + \\ & + \frac{\sin \Lambda}{R_1} y \cdot \left\{ \ln (8 R_1 \sqrt{1-y^2}) - (1-2k) - \right. \\ & \left. - \csc \Lambda \left[\ln |1 + \sin \Lambda| - (1 - \sin \Lambda) \ln |\cos \Lambda| \right] \right\} \end{aligned} \quad (7.2)$$

[†] See, for example, Ashley and Rodden (1972) and Woodward (1973).

where α is the angle of attack and k is the straight-axis location in fraction of a chord. As clearly shown, the difference between the present theory (in full line) and the panel method (in open circles) is small at most stations as compared to either of their differences from the (uncorrected) strip theory (in dash). The numerical data from the panel method are generated from a run employing 100 panels over 20 span stations. The program is a part of the NASA Ames wing-body program for a linearized compressible flow; in the computation the free-stream Mach number was set equal to $M_\infty = 0.10$, with an expected compressibility effect comparable to one percent.

A similar comparison is presented in Figure 5 for an ESP flat plate mentioned in Section 6, with same R_0 and Λ as in the last figure. Except at one station near mid-span, where the panel method gives a slightly higher value, the agreement is seen to be even better. (According to a second set of data from the panel method for the same problem based on 10 span stations with 10 panels for each span station, the noticeable discrepancy near the mid-span disappears).

7.3 Applications Involving a Lower R_1

The usefulness of an asymptotic theory based on $R_1 \gg 1$, such as the present one, will depend on its adequacy in applications where R_1 is not so large. As it is quite well known, Prandtl's success in coping with wings of lower aspect ratios lies largely in a special solution form retained in his original (1918) work. In the case of an elliptic flat plate at zero yaw, for example, the lift coefficient is obtained and computed according to the familiar form as

$$C_L = 2\pi\alpha / [1 + 2/R] \quad (7.3)$$

where $R \equiv (4/\pi) R_0$. As pointed out by Van Dyke (1964), the above result is consistent with the (second-order) asymptotic theory for high R ,

$$C_L = 2\pi\alpha \left[1 - \frac{2}{R} + \dots \right], \quad (7.4)$$

but is clearly superior than the latter in the low R range. Note that, as $R \rightarrow 0$, Prandtl's formula in rational fraction, Eq. (7.3), yields a limit which is larger than the correct slender-wing limit by a factor of 2, but Eq. (7.4) gives an infinite lift coefficient which is certainly much worse. For $R = 5-10$, or $R_0 = 4-8$, differences of Eq. (7.4) from (7.3), and from the more exact calculation, are considerable. The accuracy of the present theory is expected to be no better than its counterpart at zero yaw, Eq. (7.4), and some very definite discrepancy may therefore appear for aspect ratio below ten.

Figure 6 presents an example in the lower-aspect-ratio range in which results of span loadings of a 5:1 elliptic flat plate at 45° yaw is studied. Unlike the consistently good agreement shown in the preceding two figures, Eq. (7.2) in the present theory yields a span load (in thin full line) appreciably lower than that by the panel method (in open circles) on the forward (left) wing panel. It must be pointed out, however, that even in this instance, Eq. (7.2) is still far better than the uncorrected strip theory (in dashes). Its usefulness can be improved considerably further by recasting Eq. (7.2) into a rational fraction similar to Prandtl's original form, Eq. (7.3). Namely:

$$(S.L.) = (S.L.)_\infty / \left[2 - (S.L.)/(S.L.)_\infty \right] \quad (7.5)$$

where the subscript ∞ refers to $R_0 \rightarrow \infty$, noting that $[(S.L.)/(S.L.)_\infty - 1]$

belongs to $O(R_1^{-1})$.^{*} The result of this conversion (in heavy full line) is shown in Figure 6 where the improvement in the agreement with the panel method is seen to be, indeed, significant.

* An alternative procedure is to transform the wing upwash, say $V_o + R_1^{-1}V_i$, instead of the (S.L.), into $V_o/[1 - R_1^{-1}V_i/V_o]$. Its merit remains to be studied.

ACKNOWLEDGEMENT

The study is supported by the Office of Naval Research under Contract N00014-75-C-0520; partial support on an earlier joint study with NASA Ames Research Center Aeronautics Division (NCA2-OR 730-601) is also acknowledged. Thanks are due to S.Y. Meng for devising a method for computing the upwash function and L. Murillo for producing the exact solutions and many results in the comparison study. The author is grateful to Drs. G. Daforno and R.E. Melnik, who pointed out the earlier work by Dorodnitsyn on the same problem. Helpful discussions with R.T Jones and Ronald Smith at NASA Ames Research Center are much appreciated.

REFERENCES

- Ashley, H. and Landahl, M. 1965 Aerodynamics of Wing and Bodies, Addison Wesley, Mass. pp. 137-142.
- Ashley, H. and Rodden, W. 1972 "Wing-Body Aerodynamic Interaction", Annual Review of Fluid Mechanics, vol. 4, pp. 431-472.
- Bauer, F., Garabedian, P., Korn, D. and Jameson, A. 1974 Supercritical Wing Sections, II, Springer Verlag, pp. 11-17, pp. 192-296
- Black, R.L., Beamish, J.K. and Alexander, W.K. 1975 Wind Tunnel Investigation of an Oblique Wing Transport Model at Mach Number between 0.6 and 1.4 NASA CR-137697, HST-TR-344-0, NASA Ames Research Center, p. 11.
- Cheng, H.K. 1976 "On Lifting-Line Theory in Unsteady Aerodynamics", University of Southern California, School of Engineering, Department of Aerospace Engineering Report USCAE 133.
- Cheng, H.K. 1978 "Lifting-Line Theory of Oblique Wings", accepted for publication in AIAA Journal.
- Cheng, H.K. and Meng, S.Y. 1978a "Lifting-Line Theory of Oblique Wings in Transonic Flows", submitted to AIAA Journal.
- Cheng H.K. and Meng, S.Y. 1978b "Transonic Lifting-Line Theory of Oblique Wings and Other High-Aspect-Ratio Planforms", University of Southern California, School of Engineering, Department of Aerospace Engineering, Report USCAE 136.
- Chopra, M.G. and Kambe, T. 1977 "Hydromechanics of Lunate Tail Swimming Propulsion, pt-2", Journal Fluid Mechanics, vol. 79, pt.1, pp.49-69.
- Dorodnitsyn, A.A. 1944 "Generalization of The Lifting-Line Theory for Cases of a Wing With a Curved Axis and a Slipping Wing", Prikl. Mat. Mec. vol. 8, pp. 33-64.
- Jameson, A. and Caughey, D.A. 1977 "A Finite Volume Method for Transonic Potential Flow Calculations", AIAA paper No. 77-635, presented at AIAA 3rd Comput. Fluid Dynamics Conference, Albuquerque, New Mexico (June 27-28, 1977).
- Jones, R.T. 1950 "The Spanwise Distribution of Lift for Minimum Induced Drag of Wing Having a Given Lift and a Given Bending Moment", NACA Tech. Note 2249.
- Jones, R.T. 1972 "Reduction of Wave Drag by Asymmetrical Arrangement of Wings and Bodies", AIAA Journal, vol. 10, pp. 171-176.

REFERENCES

- Jones, R.T. 1977 "The Oblique Wing - Aircraft Design for Transonic and Low Supersonic Speeds", Acta Astronautica, vol. 4, No. 112, pp. 99-110.
- Jones, R.T. and Cohen, D. 1957 "Aerodynamics of Wings at High Speed", in Aerodynamic Components of Aircraft at High Speed, ed. by A.F. Donovan & H.R. Lawrence, Princeton University Press.
- Krienes, K. 1940 "The Elliptic Wing Based on the Potential Theory", NACA Tech. Mem. 97, translated from ZAMM, vol. 20, No. 2, pp. 65-88.
- Lighthill, M.J. 1975 Mathematical Biofluid-dynamics, Soc. Indus. Appl. Math. Philadelphia, Pa. pp. 67-92.
- Prandtl, L. 1918 "Tragflügel Theorie" Nachrichten d.k. Gesellschaft d. Wiss. zu Göttingen, Math-Phys. Klassen, pp. 451-477.
- Thurber, J.K. 1965 "An Asymptotic Method for Determining the Lift Distribution of a Swept-Back Wing of Finite Span", Comm. Pure Appl. Math., vol. 18, pp. 733-750.
- Van Dyke, M.D. 1964 Perturbation Methods in Fluid Mechanics, Academic Press pp. 167-176.
- Weisinger, J. 1947, "Über die Auftriebsverteilung von Pfeilflügeln", FB 1553, Berlin-Adlershof (1942); NACA Tech. Mem. 1120.
- Woodward, F.A. 1973 "An Improved Method for the Aerodynamic Analysis of Wing-Body-Tail Configurations in Subsonic and Supersonic Flow", NASA CR-2228, Parts I and II.

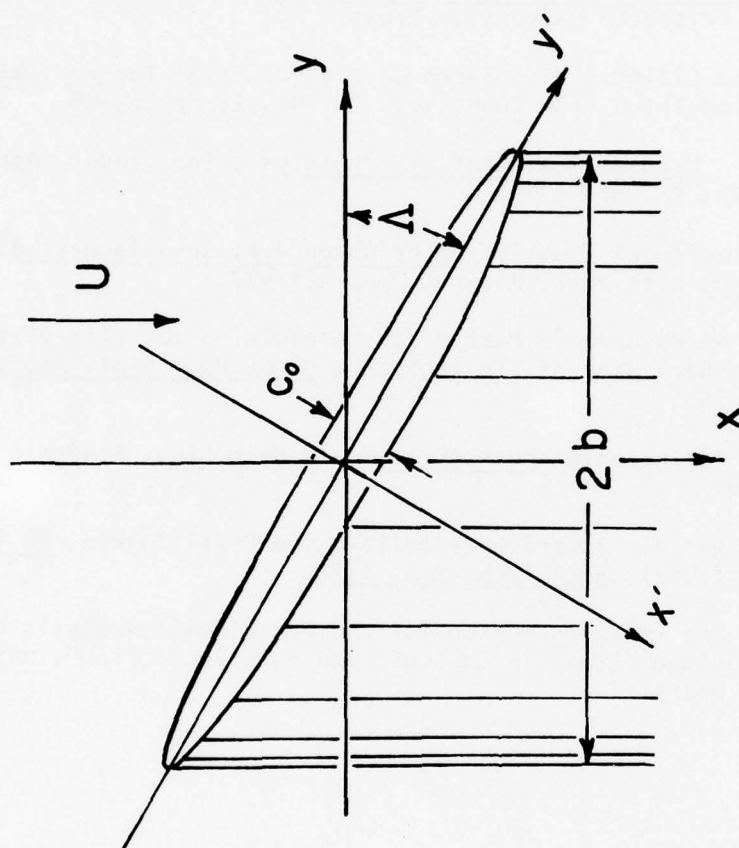


Figure 1 - Coordinates and Notations

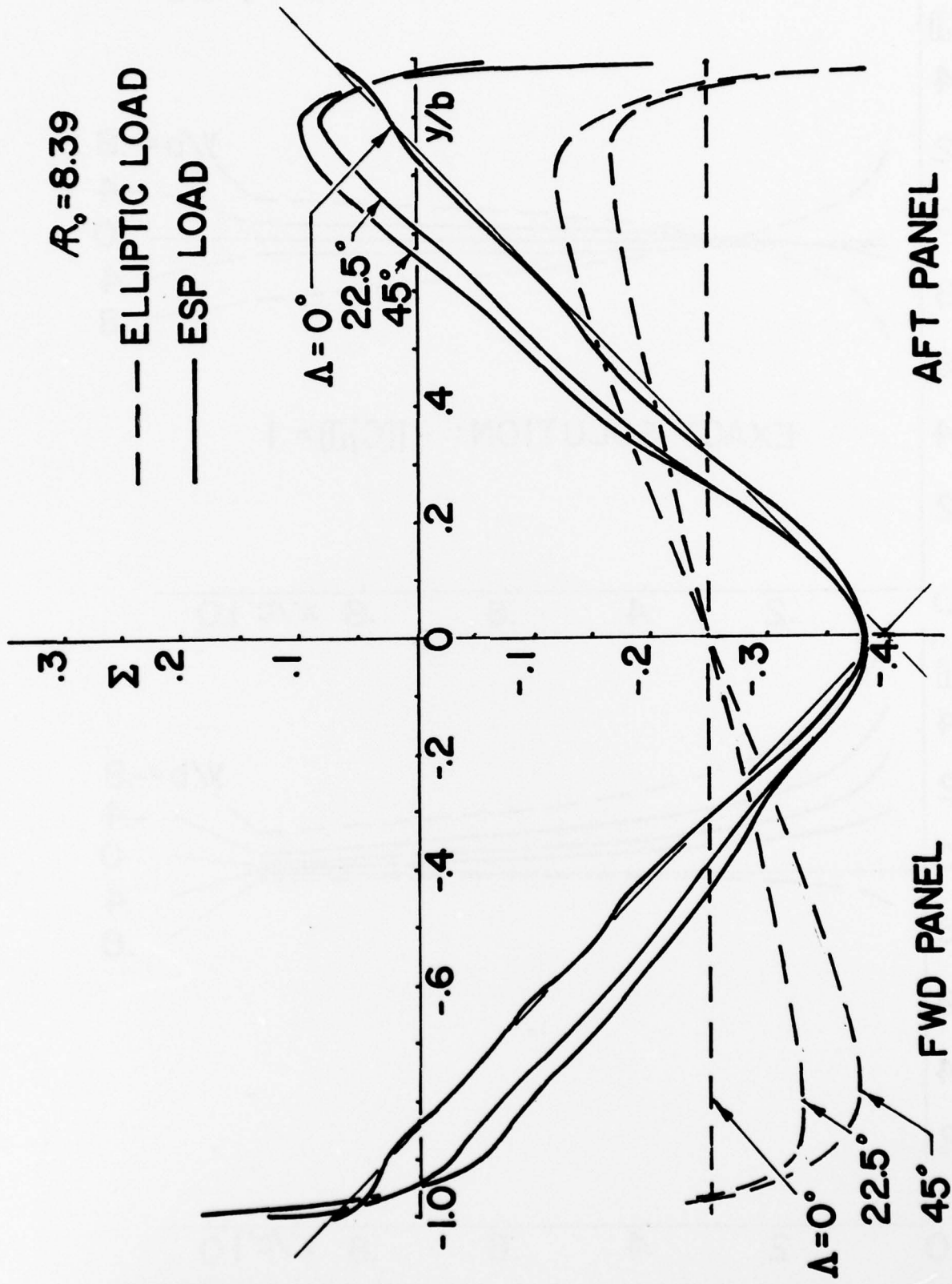


Figure 2 - The upwash function Σ illustrated for $R_o = 8.39$ at three yaw angles for an elliptic and an extended-span distribution in \bar{y} .

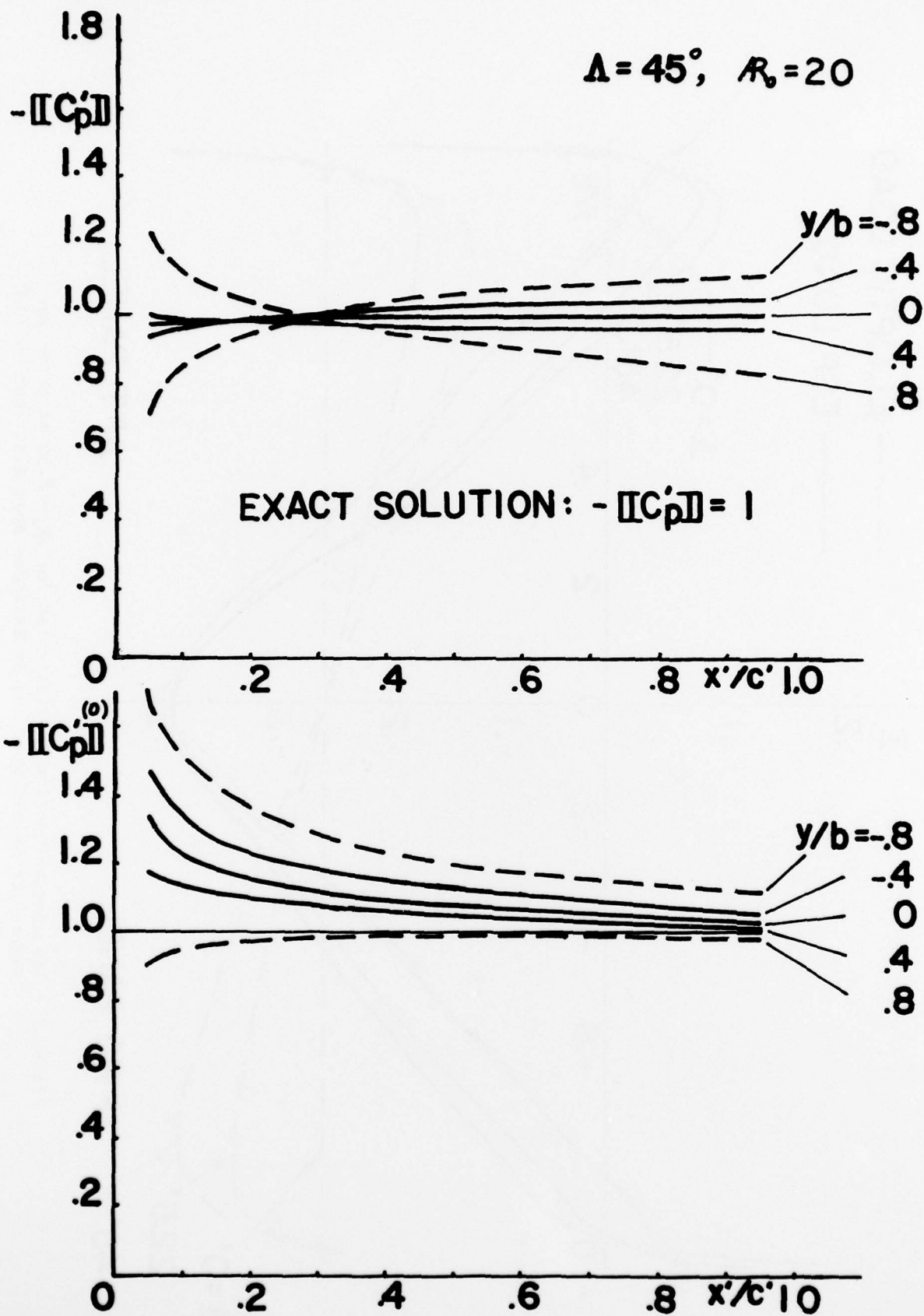


Figure 3 - Comparison of present theory with exact solution in chordwise lift distribution at various span stations.

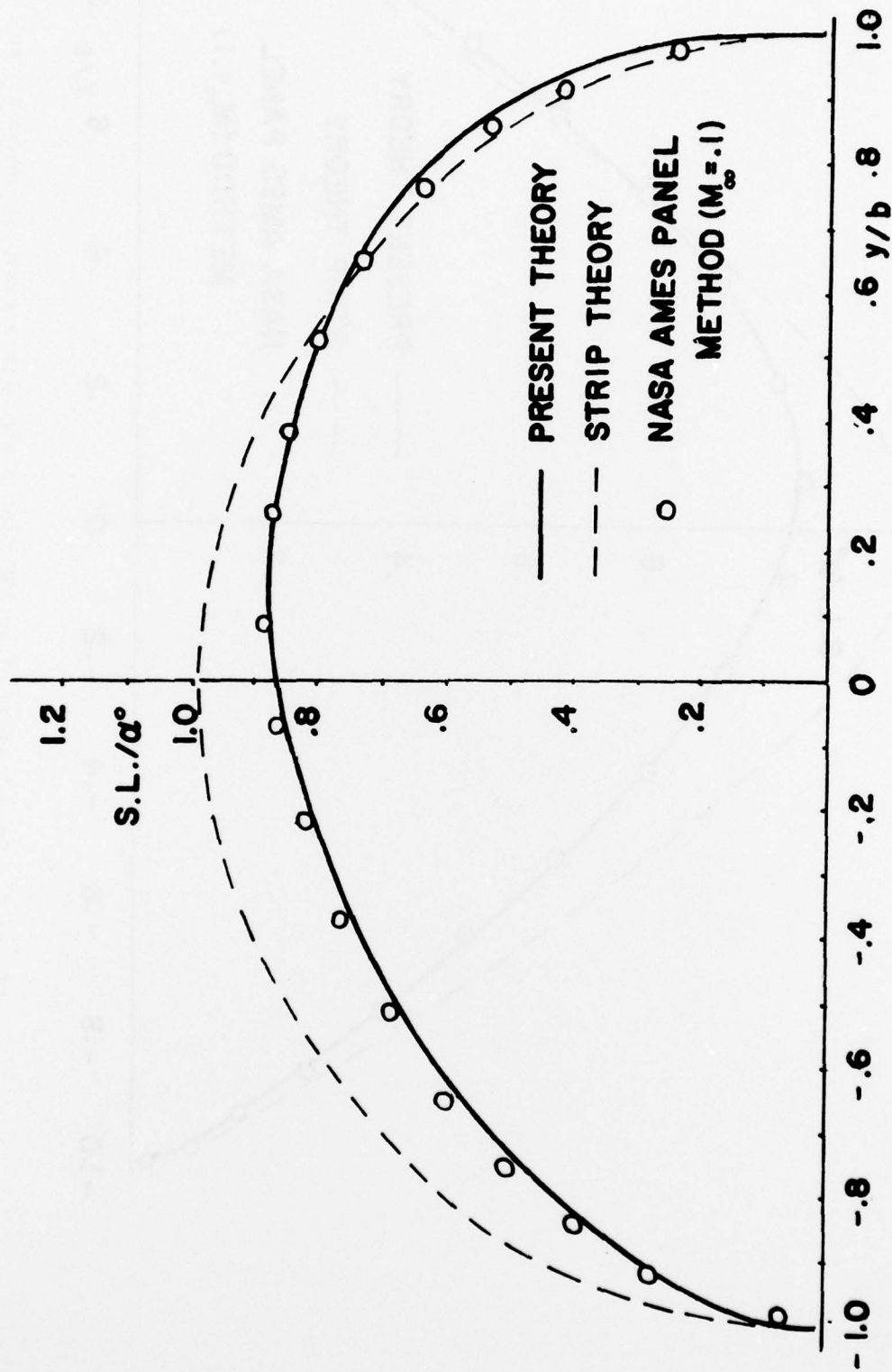


Figure 4 - Span loading of an elliptic flat plate with a ratio of unyawed span to root-chord $R_s = 16.78$ and a straight 40% chord line at 45° yaw.

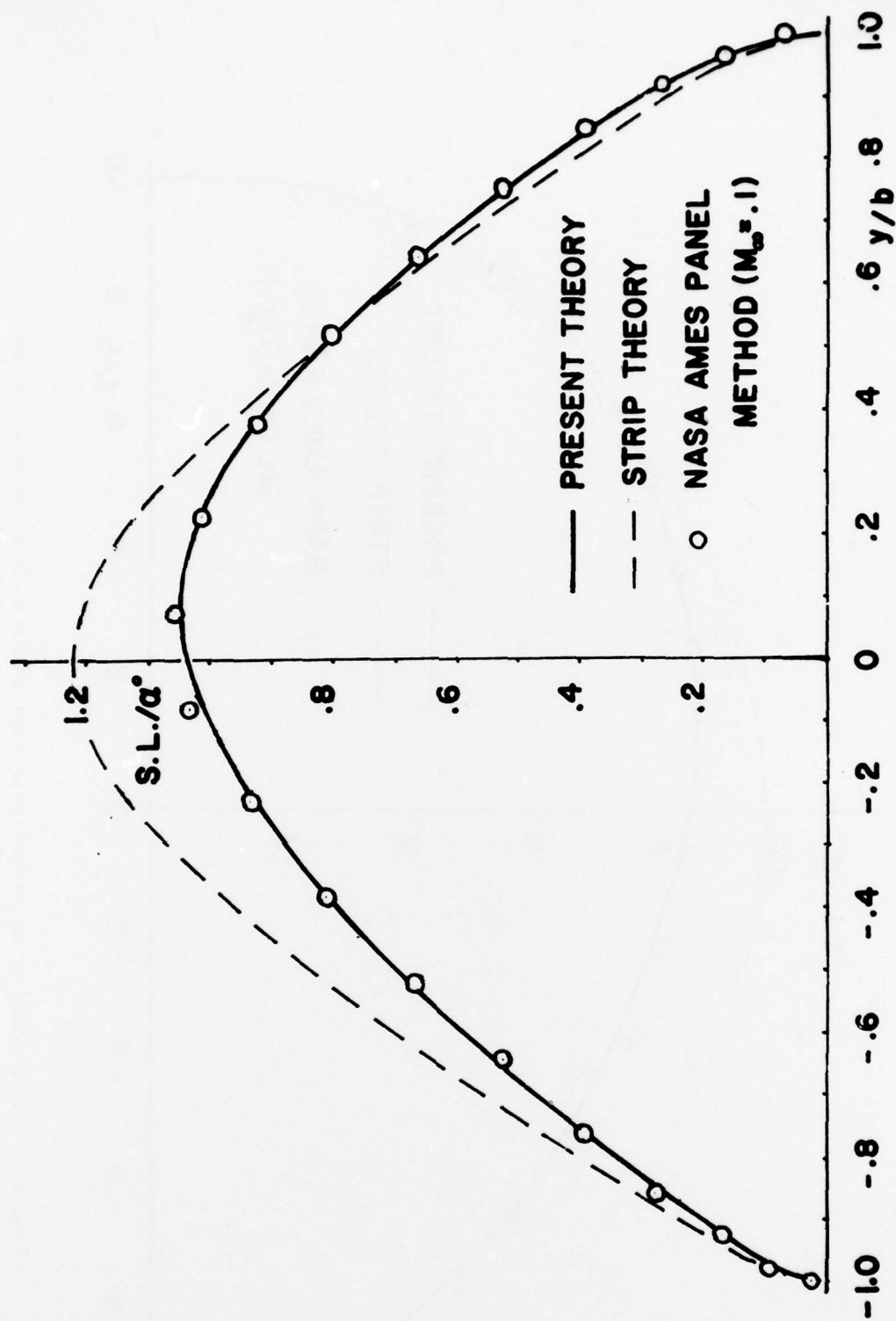


Figure 5 - Span loading of an ESP flat plate with a ratio of unyawed span to root-chord $R_c = 16.78$ and a straight 40% chord line at 45° yaw.

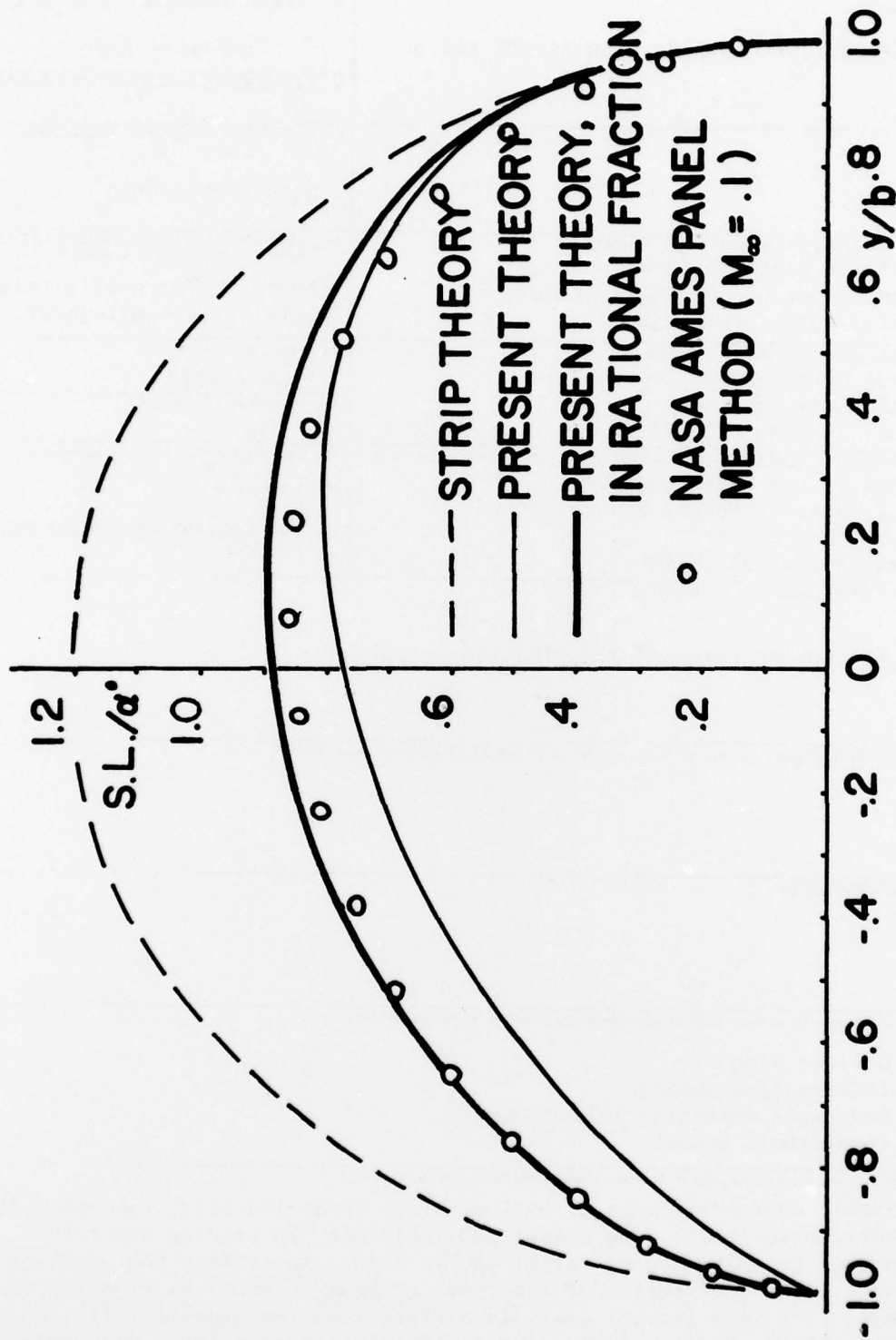


Figure 6 - Span loading of an elliptic flat plate with a ratio of unyawed span to root-chord $R_o = 5$ and a straight 50% chord line at 30° yaw.

UNCLASSIFIED

SECURITY CLASSIFICATION OF THIS PAGE (When Data Entered)

REPORT DOCUMENTATION PAGE		READ INSTRUCTIONS BEFORE COMPLETING FORM
1. REPORT NUMBER USCAE 135	2. GOVT ACCESSION NO.	3. RECIPIENT'S CATALOG NUMBER
4. TITLE (and Subtitle) THEORY OF OBLIQUE WINGS OF HIGH ASPECT RATIO		5. TYPE OF REPORT & PERIOD COVERED Technical Report
		6. PERFORMING ORG. REPORT NUMBER
7. AUTHOR(s) H. K. Cheng		8. CONTRACT OR GRANT NUMBER(s) N00014-75-C-0520
9. PERFORMING ORGANIZATION NAME AND ADDRESS University of Southern California Department of Aerospace Engineering Los Angeles, California 90007		10. PROGRAM ELEMENT, PROJECT, TASK AREA & WORK UNIT NUMBERS "Approved for public release; distribution unlimited".
11. CONTROLLING OFFICE NAME AND ADDRESS Department of the Navy, Code 438 Office of Naval Research Arlington, Virginia 22217		12. REPORT DATE August 1978
		13. NUMBER OF PAGES 33
14. MONITORING AGENCY NAME & ADDRESS (if different from Controlling Office) Department of the Navy, Code 603 Office of Naval Research, Branch Office 1030 East Green Street Pasadena, California 91106		15. SECURITY CLASS. (of this report) Unclassified
		15a. DECLASSIFICATION/DOWNGRADING SCHEDULE
16. DISTRIBUTION STATEMENT (of this Report) Approved for public release; distribution unlimited".		
17. DISTRIBUTION STATEMENT (of the abstract entered in Block 20, if different from Report)		
18. SUPPLEMENTARY NOTES		
19. KEY WORDS (Continue on reverse side if necessary and identify by block number) Oblique wing Lifting-line theory Near-wake vorticity influence Logarithmic upwash		
20. ABSTRACT (Continue on reverse side if necessary and identify by block number) The aerodynamic characteristics of oblique wings in an inviscid, incompressible flow, linearized for small wing camber and incidence, ^{are} studied under the assumption that the wing aspect ratio R_1 is high. Apart from the addition of a dominant upwash correction of the order $R_1^{-1} \ln R_1$, resulting from the sweep of the center line, the present analysis differs from the classical lifting-line theory in that the flow field next to the wing section (the inner solution) is affected by a component of the wake vorticity parallel to the center line, (continued on reverse side)		

DD FORM 1473

1 JAN 73

EDITION OF 1 NOV 65 IS OBSOLETE

UNCLASSIFIED

SECURITY CLASSIFICATION OF THIS PAGE (When Data Entered)

UNCLASSIFIED

SECURITY CLASSIFICATION OF THIS PAGE(When Data Entered)

and, hence, is not locally two-dimensional. A crucial aspect of the analysis involves the behavior of the three-dimensional corrections near the leading and trailing edges, which require special attention, lest nonuniformities arise. The results determined from matching the inner and outer solutions exhibit a strong asymmetrical spanwise influence of the wake vorticities, with a lift increase on the downstream wing panel and a lift reduction on the upstream panel. Results obtained are compared with surface-lift distributions generated by an inversed method for yawed elliptic planforms, and with span loadings generated by a panel method for elliptic flat plates (wings with zero camber) as well as an ESP (extended-span planform) wing. For R_1 in the range of 10 to 20, good agreement in the comparison is consistently found, and the improvement over the strip (local 2-D) theory is shown to be great. Recast into a rational fraction (in a form similar to that used originally by Prandtl), results obtained can be improved further and shown to be adequate for aspect ratio down to at least $R_1 = 4.33$ corresponding to a 5:1 ellipse at 30° yaw. The report also furnishes computed (finite-part of the) upwash data which will be useful in other related subsonic and transonic applications.

UNCLASSIFIED

SECURITY CLASSIFICATION OF THIS PAGE(When Data Entered)

DISTRIBUTION LIST FOR UNCLASSIFIED
TECHNICAL REPORTS AND REPRINTS ISSUED UNDER
CONTRACT NO 0014-75-C-0520 TASK LR 641-192

All addresses receive one copy unless otherwise specified

Technical Library
Building 313
Ballistic Research Laboratories
Aberdeen Proving Ground, MD 21005

Dr. F. D. Bennett
External Ballistic Laboratory
Ballistic Research Laboratories
Aberdeen Proving Ground, MD 21005

Mr. C. C. Hudson
Sandia Corporation
Sandia Base
Albuquerque, NM 81115

Professor P. J. Roache
Ecodynamics Research
Associates, Inc.
P. O. Box 8172
Albuquerque, NM 87108

Dr. J. D. Shreve, Jr.
Sandia Corporation
Sandia Base
Albuquerque, NM 81115

Defense Documentation Center
Cameron Station, Building 5
Alexandria, VA 22314 12 copies

Library
Naval Academy
Annapolis, MD 21402

Director, Tactical Technology Office
Defense Advanced Research Projects
Agency
1400 Wilson Boulevard
Arlington, VA 22209

Office of Naval Research
Attn: Code 211
800 N. Quincy Street
Arlington, VA 22217

Office of Naval Research
Attn: Code 438
800 N. Quincy Street
Arlington, VA 22217

Office of Naval Research
Attn: Code 1021P (ONRL)
800 N. Quincy Street
Arlington, VA 22217 6 copies

Dr. J. L. Potter
Deputy Director, Technology
von Karman Gas Dynamics Facility
Arnold Air Force Station, TN 37389

Professor J. C. Wu
Georgia Institute of Technology
School of Aerospace Engineering
Atlanta, GA 30332

Library
Aerojet-General Corporation
6352 North Irwindale Avenue
Azusa, CA 91702

NASA Scientific and Technical
Information Facility
P. O. Box 8757
Baltimore/Washington International
Airport, MD 21240

Dr. K. C. Wang
Martin Marietta Corporation
Martin Marietta Laboratories
1450 South Rolling Road
Baltimore, MD 21227

Dr. S. A. Berger
University of California
Department of Mechanical Engineering
Berkeley, CA 94720

Professor A. J. Chorin
University of California
Department of Mathematics
Berkeley, CA 94720

Professor M. Holt
University of California
Department of Mechanical Engineering
Berkeley, CA 94720

Dr. H. R. Chaplin
Code 1600
David W. Taylor Naval Ship Research
and Development Center
Bethesda, MD 20084

Dr. Hans Lugt
Code 184
David W. Taylor Naval Ship Research
and Development Center
Bethesda, MD 20084

Dr. Francois Frenkiel
Code 1802.2
David W. Taylor Naval Ship Research
and Development Center
Bethesda, MD 20084

Dr. G. R. Inger
Department of Aerospace Engineering
Virginia Polytechnic Institute and
State University
Blacksburg, VA 24061

Professor A. H. Nayfeh
Department of Engineering Science
Virginia Polytechnic Institute and
State University
Blacksburg, VA 24061

Mr. A. Rubel
Research Department
Grumman Aerospace Corporation
Bethpage, NY 11714

Commanding Officer
Office of Naval Research Branch Office
666 Summer Street, Bldg. 114, Section D
Boston, MA 02210

Dr. G. Hall
State University of New York at Buffalo
Faculty of Engineering and Applied
Sciences
Fluid and Thermal Sciences Laboratory
Buffalo, NY 14214

Dr. R. J. Vidal
CALSPAN Corporation
Aerodynamics Research Department
P. O. Box 235
Buffalo, NY 14221

Professor R. F. Probst
Department of Mechanical Engineering
Massachusetts Institute of Technology
Cambridge, MA 02139

Commanding Officer
Office of Naval Research Branch Office
536 South Clark Street
Chicago, IL 60605

Code 753
Naval Weapons Center
China Lake, CA 93555

Mr. J. Marshall
Code 4063
Naval Weapons Center
China Lake, CA 93555

Professor R. T. Davis
Department of Aerospace Engineering
University of Cincinnati
Cincinnati, OH 45221

Library MS 60-3
NASA Lewis Research Center
21000 Brookpark Road
Cleveland, OH 44135

Dr. J. D. Anderson, Jr.
Chairman, Department of Aerospace
Engineering
College of Engineering
University of Maryland
College Park, MD 20742

Professor W. L. Melnik
Department of Aerospace Engineering
University of Maryland
College Park, MD 20742

Professor O. Burggraf
Department of Aeronautical and
Astronautical Engineering
Ohio State University
1314 Kinnear Road
Columbus, OH 43212

Technical Library
Naval Surface Weapons Center
Dahlgren Laboratory
Dahlgren, VA 22448

Dr. F. Moore
Naval Surface Weapons Center
Dahlgren Laboratory
Dahlgren, VA 22448

Technical Library 2-51131
LTV Aerospace Corporation
P. O. Box 5907
Dallas, TX 75222

Library, United Aircraft Corporation
Research Laboratories
Silver Lane
East Hartford, CT 06108

Technical Library
AVCO-Everett Research Laboratory
2385 Revere Beach Parkway
Everett, MA 02149

Professor G. Moretti
Polytechnic Institute of New York
Long Island Center
Department of Aerospace Engineering
and Applied Mechanics
Route 110
Farmingdale, NY 11735

Professor S. G. Rubin
Polytechnic Institute of New York
Long Island Center
Department of Aerospace Engineering
and Applied Mechanics
Route 110
Farmingdale, NY 11735

Dr. W. R. Briley
Scientific Research Associates, Inc.
P. O. Box 498
Glastonbury, CT 06033

Professor P. Gordon
Calumet Campus
Department of Mathematics
Purdue University
Hammond, IN 46323

Library (MS 185)
NASA Langley Research Center
Langley Station
Hampton, VA 23665

Professor A. Chapmann
Chairman, Mechanical Engineering
Department
William M. Rice Institute
Box 1892
Houston, TX 77001

Technical Library
Naval Ordnance Station
Indian Head, MD 20640

Professor D. A. Caughey
Sibley School of Mechanical and
Aerospace Engineering
Cornell University
Ithaca, NY 14850

Professor E. L. Resler
Sibley School of Mechanical and
Aerospace Engineering
Cornell University
Ithaca, NY 14850

Professor S. F. Shen
Sibley School of Mechanical and
Aerospace Engineering
Ithaca, NY 14850

Library
Midwest Research Institute
425 Volker Boulevard
Kansas City, MO 64110

Dr. M. M. Hafez
Flow Research, Inc.
P. O. Box 5040
Kent, WA 98031

Dr. E. M. Murman
Flow Research, Inc.
P. O. Box 5040
Kent, WA 98031

Dr. S. A. Orszag
Cambridge Hydrodynamics, Inc.
54 Baskin Road
Lexington, MA 02173

Dr. P. Bradshaw
Imperial College of Science and
Technology
Department of Aeronautics
Prince Consort Road
London SW7 2BY, England

Professor T. Cebeci
California State University,
Long Beach
Mechanical Engineering Department
Long Beach, CA 90840

Mr. J. L. Hess
Douglas Aircraft Company
3855 Lakewood Boulevard
Long Beach, CA 90808

Dr. H. K. Cheng
University of Southern California,
University Park
Department of Aerospace Engineering
Los Angeles, CA 90007

Professor J. D. Cole
Mechanics and Structures Department
School of Engineering and Applied
Science
University of California
Los Angeles, CA 90024

Engineering Library
University of Southern California
Box 77929
Los Angeles, CA 90007

Dr. C. -M. Ho
Department of Aerospace Engineering
University of Southern California,
University Park
Los Angeles, CA 90007

Dr. T. D. Taylor
The Aerospace Corporation
P. O. Box 92957
Los Angeles, CA 90009

Commanding Officer
Naval Ordnance Station
Louisville, KY 40214

Mr. B. H. Little, Jr.
Lockheed-Georgia Company
Department 72-74, Zone 369
Marietta, GA 30061

Professor E. R. G. Eckert
University of Minnesota
241 Mechanical Engineering Building
Minneapolis, MN 55455

Library
Naval Postgraduate School
Monterey, CA 93940

Supersonic-Gas Dynamics Research
Laboratory
Department of Mechanical Engineering
McGill University
Montreal 12, Quebec, Canada

Dr. S. S. Stahara
Nielsen Engineering & Research, Inc.
510 Clyde Avenue
Mountain View, CA 94043

Engineering Societies Library
345 East 47th Street
New York, NY 10017

Professor A. Jameson
New York University
Courant Institute of Mathematical
Sciences
251 Mercer Street
New York, NY 10012

Professor G. Miller
Department of Applied Science
New York University
26-36 Stuyvesant Street
New York, NY 10003

Office of Naval Research
New York Area Office
715 Broadway - 5th Floor
New York, NY 10003

Dr. A. Vaglio-Laurin
Department of Applied Science
26-36 Stuyvesant Street
New York University
New York, NY 10003

Professor H. E. Rauch
Ph.D. Program in Mathematics
The Graduate School and University
Center of the City University of
New York
33 West 42nd Street
New York, NY 10036

Librarian, Aeronautical Library
National Research Council
Montreal Road
Ottawa 7, Canada

Lockheed Missiles and Space Company
Technical Information Center
3251 Hanover Street
Palo Alto, CA 94304

Commanding Officer
Office of Naval Research Branch Office
1030 East Green Street
Pasadena, CA 91106

California Institute of Technology
Engineering Division
Pasadena, CA 91109

Library
Jet Propulsion Laboratory
4800 Oak Grove Drive
Pasadena, CA 91103

Professor H. Liepmann
Department of Aeronautics
California Institute of Technology
Pasadena, CA 91109

Mr. L. I. Chasen, MGR-MSD Lib.
General Electric Company
Missile and Space Division
P. O. Box 8555
Philadelphia, PA 19101

Mr. P. Dodge
Airesearch Manufacturing Company
of Arizona
Division of Garrett Corporation
402 South 36th Street
Phoenix, AZ 85010

Technical Library
Naval Missile Center
Point Mugu, CA 93042

Professor S. Bogdonoff
Gas Dynamics Laboratory
Department of Aerospace and
Mechanical Sciences
Princeton University
Princeton, NJ 08540

Professor S. I. Cheng
Department of Aerospace and
Mechanical Sciences
Princeton University
Princeton, NJ 08540

Dr. J. E. Yates
Aeronautical Research Associates
of Princeton, Inc.
50 Washington Road
Princeton, NJ 08540

Professor L. Sirovich
Division of Applied Mathematics
Brown University
Providence, RI 02912

Dr. P. K. Dai (RI/2178)
TRW Systems Group, Inc.
One Space Park
Redondo Beach, CA 90278

Redstone Scientific Information Center
Chief, Document Section
Army Missile Command
Redstone Arsenal, AL 35809

U.S. Army Research Office
P. O. Box 12211
Research Triangle, NC 27709

Editor, Applied Mechanics Review
Southwest Research Institute
8500 Culebra Road
San Antonio, TX 78228

Library and Information Services
General Dynamics-CONVAIR
P. O. Box 1128
San Diego, CA 92112

Dr. R. Magnus
General Dynamics-CONVAIR
Kearny Mesa Plant
P. O. Box 80847
San Diego, CA 92138

Mr. T. Brundage
Defense Advanced Research Projects
Agency
Research and Development Field Unit
APO 146, Box 271
San Francisco, CA 96246

Office of Naval Research
San Francisco Area Office
One Hallidie Plaza, Suite 601
San Francisco, CA 94102

Library
The RAND Corporation
1700 Main Street
Santa Monica, CA 90401

Dr. P. E. Rubbert
Boeing Aerospace Company
Boeing Military Airplane Development
Organization
P. O. Box 3707
Seattle, WA 98124

Dr. H. Yoshihara
Boeing Aerospace Company
P. O. Box 3999
Mail Stop 41-18
Seattle, WA 98124

Mr. R. Feldhuhn
Naval Surface Weapons Center
White Oak Laboratory
Silver Spring, MD 20910

Librarian
Naval Surface Weapons Center
White Oak Laboratory
Silver Spring, MD 20910

Dr. J. M. Solomon
Naval Surface Weapons Center
White Oak Laboratory
Silver Spring, MD 20910

Professor J. H. Ferziger
Department of Mechanical Engineering
Stanford University
Stanford, CA 94305

Professor K. Karamcheti
Department of Aeronautics and
Astronautics
Stanford University
Stanford, CA 94305

Professor M. van Dyke
Department of Aeronautics and
Astronautics
Stanford University
Stanford, CA 94305

Professor O. Bunemann
Institute for Plasma Research
Stanford University
Stanford, CA 94305

Engineering Library
McDonnell Douglas Corporation
Department 218, Building 101
P. O. Box 516
St. Louis, MO 63166

Dr. R. J. Hakkinen
McDonnell Douglas Corporation
Department 222
P. O. Box 516
St. Louis, MO 63166

Dr. R. P. Heinisch
Honeywell, Inc.
Systems and Research Division -
Aerospace Defense Group
2345 Walnut Street
St. Paul, MN 55113

Dr. N. Malmuth
Rockwell International Science Center
1049 Camino Dos Rios
P. O. Box 1085
Thousand Oaks, CA 91360

Library
Institute of Aerospace Studies
University of Toronto
Toronto 5, Canada

Professor W. R. Sears
Aerospace and Mechanical Engineering
University of Arizona
Tucson, AZ 85721

Professor A. R. Seebass
Department of Aerospace and Mechanical
Engineering
University of Arizona
Tucson, AZ 85721

Dr. K. T. Yen
Code 3015
Naval Air Development Center
Warminster, PA 18974

Air Force Office of Scientific Research
(SREM)
Building 1410, Bolling AFB
Washington, DC 20332

Chief of Research and Development
Office of Chief of Staff
Department of the Army
Washington, DC 20310

Library of Congress
Science and Technology Division
Washington, DC 20540

Director of Research (Code RR)
National Aeronautics and Space
Administration
600 Independence Avenue, SW
Washington, DC 20546

Library
National Bureau of Standards
Washington, DC 20234

National Science Foundation
Engineering Division
1800 G Street, NW
Washington, DC 20550

Mr. W. Koven
AIR 03E
Naval Air Systems Command
Washington, DC 20361

Mr. R. Siewert
AIR 320D
Naval Air Systems Command
Washington, DC 20361

Technical Library Division
AIR 604
Naval Air Systems Command
Washington, DC 20361

Code 2627
Naval Research Laboratory
Washington, DC 20375

SEA 03512
Naval Sea Systems Command
Washington, DC 20362

SEA 09G3
Naval Sea Systems Command
Washington, DC 20362

Dr. A. L. Slafkosky
Scientific Advisor
Commandant of the Marine Corps
(Code AX)
Washington, DC 20380

Director
Weapons Systems Evaluation Group
Washington, DC 20305

Chief of Aerodynamics
AVCO Corporation
Missile Systems Division
201 Lowell Street
Wilmington, MA 01887

Research Library
AVCO Corporation
Missile Systems Division
201 Lowell Street
Wilmington, MA 01887

AFAPL (APRC)
AB
Wright Patterson, AFB, OH 45433

Dr. Donald J. Harney
AFFDL/FX
Wright Patterson AFB, OH 45433